C. Gao et alii, Frattura ed Integrità Strutturale, 33 (2015) 471-484; DOI: 10.3221/IGF-ESIS.33.52

A new micromechanical model of CNT-metal nanocomposites with random clustered distribution of CNTs

Chongyang Gao, Yu Lu
School of Mechanical Engineering, Zhejiang University, Hangzhou 310027, China
corresponding author: gcysci@163.com

Y.T. Zhu
2School of Materials Science and Engineering, Nanjing University of Science and Technology, Nanjing 210094, China

ABSTRACT. Uniform dispersion of carbon nanotubes (CNTs) is a key issue for utilization of their reinforcement potential in CNT-reinforced metal matrix nanocomposites (MMNCs). It was reported that CNT clusters often exist in MMNCs prepared by various techniques, which reduces the load transfer efficiency between the matrix and reinforcement. In this paper, a new micromechanical constitutive model of CNT-reinforced MMNCs is developed, which takes into account of the influences of CNT clusters and misorientations. The strength values of a CNT/Al nanocomposite predicted by the new model are compared first with experimental data for validation. Then, the developed model is applied to predict the size effect, temperature effect and strain rate effect of the nanocomposite in its overall elastoplastic response.

KEYWORDS. Micromechanical modelling; Metal matrix nanocomposites; Carbon nanotubes; Cluster effect; Misorientation angle.

INTRODUCTION

In recent years, it has been reported that incorporating carbon nanotubes (CNTs) into polymers [1-3], ceramics and metals [4-7] can dramatically improve their mechanical properties. This is due to the high strength; high Young's modulus and super thermal conductivity of CNTs. Metal matrix nanocomposites (MMNCs) reinforced with CNTs have enhanced yield strength and a low thermal expansion coefficient, which render them substantial potential in some weight sensitive applications such as aerospace structures [8]. Yang et al. [9] demonstrated that the yield strength of a 1.5 wt. % CNT/Al nanocomposite produced by an improved chemical vapor deposition (CVD) is 2.2 times that of the pure aluminum, while the result obtained in compression tests [10] is not so high due to different preparation technique of the sample. Kim et al. [11] showed that the measured tensile strength of CNT/Cu nanocomposite with 10 vol. % CNTs is 281MPa, which is approximately 1.6 times higher than that of unreinforced pure copper. Li et al. [12] made CNT-nanocrystalline Cu nanoacomposite using ball-milling and high-pressure torsion consolidation, which has very high yield strength of 1100 MPa at 1 wt% CNT addition. Thus, CNTs can be an ideal reinforcement for material design to improve mechanical properties of composites.

The high aspect ratio of length to diameter of curved CNTs makes them prone to entangle with each other resulting in clustering in matrix, and consequently difficult to be uniformly dispersed in matrix. To solve this problem, various preparation techniques have been employed to achieve a more uniform distribution of CNTs in MMNCs so as to realize

their full strengthening potential. However, agglomeration and imperfect interfacial load transfer of CNTs still often exist in these composites. To facilitate the applications of CNT-reinforced metal matrix nanocomposites, it is essential to develop a reliable micromechanical constitutive model that can be used to describe and predict their mechanical properties. Some modeling efforts have been made to describe the mechanical properties of the CNT-reinforced nanocomposites. Courtney [13] established a classic model for short-fiber-reinforced plastic-matrix composites by introducing the effect of the aspect ratio into the basic role-of-mixture model, which can be applicable to CNT-reinforced nanocomposites. Based on the generalized shear-lag model [14] for metal matrix composites with reinforcement in cylindrical forms, Kim et al. [11] proposed a strength model to describe a two-stage yielding process in the experimental stress–strain curves of the CNT/Cu nanocomposites, and also observed elongated CNT clusters in the microstructure of the composite. Barai and Weng [15] developed a two-scale micromechanical model to make a pioneering analysis of the effect of CNT agglomeration and interface condition on the strength of CNT-reinforced MMNCs. Obviously, it is inevitable that a lot of CNT agglomerations in metallic matrix materials will appear because of easy entanglement of CNTs, especially for those with the high aspect ratio, as observed in [16-18]. Although there are also some other models proposed for CNT-reinforced polymers matrix nanocomposites [1, 3, 19, 20], a model with consideration of clustering phenomenon is still lacking.

To describe the flow stress and estimate the plastic strength of CNT-reinforced metal matrix composites, a new micromechanical constitutive model, with consideration of the effect of CNT clusters and the influence of CNT misorientation angle, will be proposed in this paper. In the "Modelling of CNT-reinforced MMNCs" section, the cluster effect is introduced into the new model by using the statistically average equivalent length and diameter of CNTs, and the misorientation angle effect is reflected by a definition of an effective load transfer coefficient. In the next section, the model parameters are determined for the CNT/Al nanocomposite by a nonlinear multi-variable global optimization method, i.e., generic algorithm. In the "Results and discussion" section, the new model is experimentally validated, and some important predictions of the model are given and discussed.

MODELLING OF CNT-REINFORCED MMNCS

Macroscopically, the CNT reinforced metal matrix nanocomposite is deformed homogeneously, in which the metal matrix is plastic and the CNT fiber is elastic. The MMNCs derive their plasticity from the good plastic behavior of the metallic matrix materials. The flow stress of CNT-reinforced MMNCs during the elastoplastic deformation process can be generally expressed below with the classical rule of mixtures as widely used for two-phase composites [20]:

$$\sigma_c = v_f \sigma_f + \left(1 - v_f\right)\sigma_m \tag{1}$$

where σ_c the flow stress of nanocomposites is, σ_f is the stress of CNTs at composite failure, σ_m is the flow stress of the pure matrix material. v_f denotes the volume fraction of CNTs.

For MMNCs reinforced with discontinuous CNTs, the applied load transfers from the matrix to CNTs along the CNT–matrix interface by the way of shear stress, and interfacial bonding significantly affects the strength of the composite. In order to load high-strength fibers to their maximum strength, the metallic matrix will flow plastically in response to the high shear stress developed. Plastic deformation of a matrix implies that the shear stress at the interface will never go above the matrix shear yield strength. In such a case, the following equation can be derived on a perfect bonding interface based on the equilibrium of forces [13]:

$$\sigma_{fm}\pi\frac{D^2}{4} = \tau_{iy}\pi D\frac{l}{2} \tag{2}$$

where τ_{iy} is the shear yield strength of the interface and σfm is the maximum stress in CNTs, l and D are the average length and diameter of primary CNTs, respectively. It can be seen that the maximum stress in CNTs varies with the length of CNTs. If a carbon nanotube is sufficiently long, it should be possible to load the CNT to its breaking stress, $\sigma_{fm} = \sigma_{fb}$, by means of load transfer through the metallic matrix flowing plastically around it. That is to say, there exists a critical

length of CNTs, l^{cr}, which is the minimum length necessary to reach fracture for a given CNT diameter. Based on Eq. (2), the critical length of CNTs can be deduced as:

$$l^{cr} = \frac{D}{2\tau_{iy}}\sigma_{fb} \tag{3}$$

If $l < l^{cr}$, the matrix will flow plastically around CNTs and load a CNT to a stress in its central position given by $\sigma_f = 2(l/D)\tau_{my}$. For $l \geq l^{cr}$, the average stress in a CNT can be written as:

$$\begin{aligned}\bar{\sigma}_f &= \frac{1}{l}\int_0^l \sigma_f(x)dx \\ &= \frac{1}{l}[\phi\sigma_f l^{\mathrm{cr}} + \sigma_f(l - l^{\mathrm{cr}})] \\ &= [1 - \frac{l^{\mathrm{cr}}}{l}(1-\phi)]\sigma_f\end{aligned} \tag{4}$$

where ϕ can be regarded as a load transfer function and $\phi\sigma_f$ represents the average stress of CNTs over a portion l^{cr}. The value of ϕ will be precisely 1/2 for an ideally plastic matrix with no strain hardening, i.e., the increase in stress in a CNT over the portion was assumed as being linear. Now, by amending the CNT stress in Eq. (1) with the average stress in Eq. (4), a basic model of CNT-reinforced MMNCs can be obtained as:

$$\sigma_c = \left(1 - \frac{1}{4}\frac{\sigma_{fb}}{\tau_{iy}}\frac{D}{l}\right)\nu_f\sigma_f + \left(1-\nu_f\right)\sigma_m \tag{5}$$

Thermo-Viscoplastic constitutive model of fcc metal matrix materials

For CNT reinforced MMNCs, the reported matrices are mostly the lightweight metal materials such as aluminum, copper, magnesium and their alloys. Although the carbon nanotubes are dispersed in the matrices to enhance their mechanical properties, the matrix materials play the most significant role in the plastic deformation behavior of the CNT reinforced composites. To reasonably describe the plastic deformation behaviors of the composite, a reliable plastic constitutive model should be established for the metallic matrix material.

The plastic deformation of metals can be explained as the process of dislocation motion and accumulation under the rate-controlled and thermally-activated mechanism. In the thermal activation analysis, dislocation motion is resisted by both short-range and long-range barriers. The short-range barriers may be overcome by thermal activation, while the long-range barriers are essentially not related with temperature (i. e. it is athermal). Hence, the flow stress of the metal materials, which is essentially defined by the material resistance to dislocation motion, can be decomposed into two parts:

$$\sigma_m = \sigma_{ath} + \sigma_{th} \tag{6}$$

where σ_m is the flow stress of the matrix material; σ_{ath} is the athermal component of the flow stress reflecting the long-range barriers, while σ_{th} is the thermal component of the flow stress reflecting the short-range barriers which depends on the thermal activation. By using the mechanical threshold stress (MTS, denoted as $\hat{\sigma}$) as a reference stress that characterizes the constant structure of a material, the thermal stress can be expressed as:

$$\sigma_{th} = f\left(\dot{\varepsilon}, T\right)\cdot\hat{\sigma}_{th} \tag{7}$$

where $\hat{\sigma}_{th}$ is the thermal component of MTS according to $\hat{\sigma} = \hat{\sigma}_{ath} + \hat{\sigma}_{th}$, $f\left(\dot{\varepsilon}, T\right)$ is the thermal activation function (<1.0) representing the coupling effects of strain rate ($\dot{\varepsilon}$) hardening and temperature (T) softening. Based on the well-known relation of dislocation speed and thermal activation energy (or called free energy) proposed by Johnston and

Giman [21] and the expression of free energy given by Kocks and Ashby [22], the thermal activation function can be expressed as:

$$f\left(\dot{\varepsilon},T\right)=\left\{1-\left[-\xi_2 T\ln\left(\frac{\dot{\varepsilon}}{\dot{\varepsilon}_0}\right)\right]^{1/q}\right\}^{1/p} \tag{8}$$

On the other hand, with consideration of the effect of grain size in the flow stress by using the Hall-Petch relationship, the athermal stress can be written as:

$$\sigma_{ath}=\sigma_G+\tilde{k}d^{-1/2} \tag{9}$$

where σ_G is the stress due to initial defect, d is the grain size and $\tilde{k}$ is a microstructural stress modulus. The athermal stress can be treated as a constant as a whole because the grain size can be measured for a particular matrix.

For a face-centered cubic (fcc) matrix (e.g., pure aluminum and its alloys), the thermal component of MTS has been deduced in [23]. Finally, the constitutive model of fcc metal matrix materials was determined as:

$$\sigma_m=\sigma_{ath}+\hat{Y}\varepsilon^n\exp\left[\xi_1 T\ln\left(\frac{\dot{\varepsilon}}{\dot{\varepsilon}_{s0}}\right)\right]\left\{1-\left[-\xi_2 T\ln\left(\frac{\dot{\varepsilon}}{\dot{\varepsilon}_0}\right)\right]^{1/q}\right\}^{1/p} \tag{10}$$

where $\hat{Y}$ is the reference thresholds of the thermal stress; n is strain hardening exponent; $\xi_1=\hat{k}/\left(g_{s0}G_m b^3\right)$ and $\xi_2=\hat{k}/\left(g_0 G_m b^3\right)$ (here $\hat{k}$ is the Boltzmann constant, g_0 and g_{s0} are the normalized and saturated free energies, G_m is the shear modulus of the matrix material, b is the Burgers vector representing the excursion induced by dislocation); $\dot{\varepsilon}_0$ and $\dot{\varepsilon}_{s0}$ are the reference and saturated strain rates; q and p are a pair of parameters representing the shape of crystal potential barrier.

Compared with the conventional modelling of matrix materials which just adopt the yield strength of the matrix [10, 18], the new model of matrix materials is a physics-based thermo-viscoplastic constitutive relation that can describe the plastic flow stress of CNT reinforced MMNCs during plastic deformation with consideration of strain rate hardening and temperature softening effects.

Consideration of the misorientation angel of CNTs

Because CNTs are randomly distributed in matrix and are highly curved when dispersed in matrix, the misorientation angle, θ, between the loading direction and the nanotube length direction for a CNT always varies along its length. To reflect the influence of misorientation angle of CNTs in the constitutive model, it was assumed that the curved CNTs can be regarded as a chain of multiple straight segments, as shown in Figure 1.

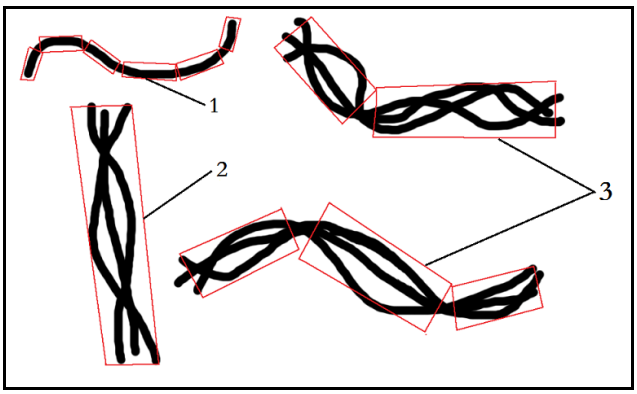

Figure 1: Cutting of the curved CNTs as a chain of short straight ones (case 1- single curved CNTs; case 2- straight clustered CNTs; case 3- curved clustered CNTs).

For CNT-reinforced MMNCs fabricated by hot extrusion, an exponential function was proposed as the probability density function of the distribution of misorientation angle [14]:

$$f(\theta) = B\exp(-k\theta) \tag{11}$$

where B is a constant, and k is a constant dependent on the alignment of CNTs. Now, if the effective strengthening stress of CNTs can be expressed as $\tilde{\lambda}\sigma_f$ (where $\tilde{\lambda}$ is an effective load transfer coefficient defined with the misorientation distribution function), the basic model of CNT-reinforced MMNCs in Eq. (5) may be improved as one with consideration of the influence of misorientation angle. However, the definition of the load transfer coefficient is always assumed in an empirical approach and lacks physical basis of constitutive modelling. In addition, the average length of the CNTs dispersed in MMNCs is generally less than the critical length, which is estimated as several dozens of micrometers. So the model in Eq. (5) may be not suitable for further modelling of the misorientation angle effect. Therefore, a physically-based model of short fibre-reinforced composites [24] was introduced below, so as to calculate the direct strengthening of CNTs for CNT-reinforced MMNCs with a known distribution of misorientation angle and under the assumption that perfect bonding exists between fibers and the matrix.

For simplicity, an isotropic Poisson's ratio, υ, was assumed for the composite. Since CNTs with smaller inclination angles from the loading direction bear larger stresses and break first during tensile loading, we assumed that θ_0 is a critical inclination angle within which every CNT has been broken, i.e., CNTs with the inclination angle θ_0 bear a stress equal to their ultimate strength and are just about to break. Then, the stress in a CNT can be derived as [24]

$$\sigma(\theta) = \begin{cases} 0 & 0 \le \theta < \theta_0 \\ \dfrac{\cos^2\theta - \upsilon\sin^2\theta}{\cos^2\theta_0 - \upsilon\sin^2\theta_0}\sigma_f & \theta_0 \le \theta < \theta_f \\ -\dfrac{(\cos^2\theta - \upsilon\sin^2\theta)}{\cos^2\theta_0 - \upsilon\sin^2\theta_0}\sigma_f & \theta_f \le \theta \le \dfrac{\pi}{2} \end{cases} \tag{12}$$

where θ_f is known as $\sin^2\theta_f = 1/(1+\upsilon)$.

To obtain the total load, $P(\theta)$ at a specimen cross-section, A, perpendicular to the loading direction, the orientation-density distribution of CNTs intercepted by the cross-section, $n_c(\theta)$, is also needed and deduced as

$$n_c(\theta) = \frac{A}{a_f}v_f\left\{1\text{-}\frac{D}{l}\sqrt{\left(\frac{1}{\sqrt{v_f}}-1\right)\cdot\frac{E_f}{G_m}}\right\}f(\theta)\cos\theta \tag{13}$$

where $a_f = \pi D^2/4$, E_f is Young's modulus of CNTs, G_m is the shear modulus of the matrix. $f(\theta)$ is the misorientation distribution of three-dimensional randomly-oriented CNTs. The exponential function proposed in Eq. (11) was adopted here for the distribution, as distinct from the previously used ones.

The total load is a function of θ_0 and can be calculated as

$$P(\theta_0) = \int_{\theta_0}^{\pi/2} n_c(\theta)\sigma(\theta)a_f\cos\theta d\theta \tag{14}$$

Its maximum value at $\theta_0 = 0$ can be considered as the load that CNTs can carry at composite failure. Thus, by substituting Eqs. (12) and (13) into Eq. (14), the strengthening stress ($\Delta\sigma$) contributed directly by CNTs can be finally integrated as

$$\Delta\sigma = \frac{P(\theta_0)_{\max}}{A} = R(\theta_f)\left\{1-\frac{D}{l}\sqrt{\left(\frac{1}{\sqrt{v_f}}-1\right)\cdot\frac{E_f}{G_m}}\right\}v_f\sigma_f \tag{15}$$

where

$$R(\theta_f) = B[W(0)+W(\pi/2)-2W(\theta_f)] \tag{16}$$

and

$$W(\theta) = \left\{\frac{3-\upsilon}{8k}+\left[\frac{k}{8(k^2+16)}\cos(4\theta)-\frac{1}{2(k^2+16)}\sin(4\theta)\right](1+\upsilon)\right. \\ \left.+\frac{k}{2(k^2+4)}\cos(2\theta)-\frac{1}{k^2+4}\sin(2\theta)\right\}e^{-k\theta} \tag{17}$$

Model modification with consideration of CNT cluster effect

As seen in Figure 2, CNTs always agglomerate in the metallic matrix and form a lot of clusters [16], though various techniques were used to make the dispersion of reinforcement as uniform as possible. This is why the strength of the nanocomposite measured in tests is actually far lower than the prediction of theoretical models.

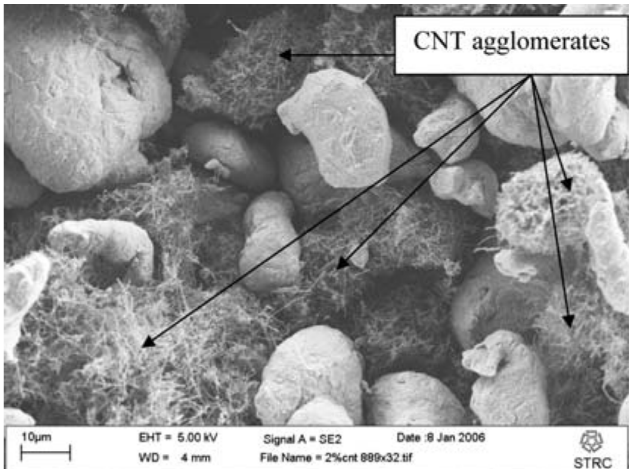

Figure 2 Clusters of carbon nanotubes after dry mixing of CNTs and Al powders [16] (with kind permission from Springer Science and Business Media).

As summarized in the Introduction, most models of CNT reinforced MMNCs were established with the assumption that the CNTs are uniformly distributed in the matrix as shown in Figure 3(a). However, there exists serious cluster phenomenon of CNTs in general as shown in Fig. 3(b). Therefore, a modified constitutive model of CNTs reinforced MMNCs with consideration of the cluster effect was specially proposed as follows.

It was proved by the experimental observation by Luo et al. [25] that the free-path spacing of CNTs follows a logarithmic normal distribution. And Tyson et al. [26] pointed out that the particle size of clustered CNTs also follows the lognormal distribution, and proved in their experiments that the lognormal distribution has the same mean value and standard deviation as the associated normal distribution. In our modelling, a CNT cluster, which is resulted from a group of intertwined CNTs, was regarded as an equivalent large reinforced particle, the shape of which can be approximately described by an equivalent length (l_c) and an equivalent diameter (D_c) as shown in Figure 3(b). So, the two sizes should follow the lognormal distribution, respectively. Their probability density functions of the lognormal distribution can be written as follows:

$$f(x)=\frac{1}{\sqrt{2\pi}nx}\exp\left[-\frac{1}{2}\left(\frac{\ln x-m}{n}\right)^2\right],\ x>0\quad (x=l_c,D_c) \tag{18}$$

and

$$\begin{cases} m_i=\ln\dfrac{\alpha_i^{\,2}}{\sqrt{\alpha_i^{\,2}+\beta_i^{\,2}}} \\ n_i=\sqrt{\ln\dfrac{\alpha_i^{\,2}+\beta_i^{\,2}}{\alpha_i^{\,2}}} \end{cases},\qquad (i=l_c,D_c) \tag{19}$$

where α_l and α_D represent the mean values of the associated normal distribution of the equivalent length and diameter, respectively; β_l and β_D represent the standard deviations of the associated normal distribution of the equivalent length and diameter, respectively.

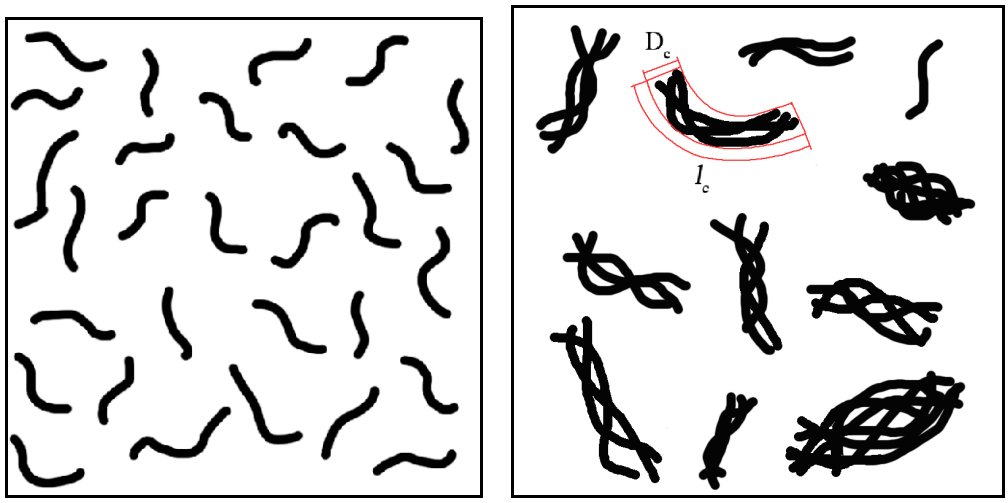

Figure 3: Comparison of random distributions of CNTs (a) uniform pattern; (b) with clusters

According to the lognormal distribution of the equivalent length and diameter of CNTs in Eq. (18), the average values of the equivalent length ($\bar{l}_c$) and diameter ($\bar{D}_c$) of CNTs can be statistically calculated as:

$$\bar{l}_c=\int_{l_{c,\min}}^{l_{c,\max}} l_c\cdot f\left(l_c\right)dl_c=e^{m_{l_c}+\frac{n_{l_c}^2}{2}} \tag{20}$$

$$\bar{D}_c=\int_{D_{c,\min}}^{D_{c,\max}} D_c\cdot f(D_c)dD_c=e^{m_{D_c}+\frac{n_{D_c}^2}{2}} \tag{21}$$

where $l_{c,\max}$ and $D_{c,\max}$ are the maximum values of the equivalent length and diameter of the CNT clusters; $l_{c,\min}$ and $D_{c,\min}$ are the minimum values of them. The upper and lower boundaries of the equivalent length and diameter following the lognormal distribution were illustrated in Figure 4. Obviously, there exist minimum and maximum boundary values for the equivalent length and diameter in reality. The minimum values can be regarded as several times of the average original length and diameter of CNTs (about 15 times as presented in [16]), and the maximum values can be evaluated by

experimental observations like Figure 2. In addition, the standard deviations of the associated normal distribution of the equivalent length and diameter will be eliminated in their average values of lognormal distribution under the presupposed condition in Eq. (19) for the lognormal distribution.

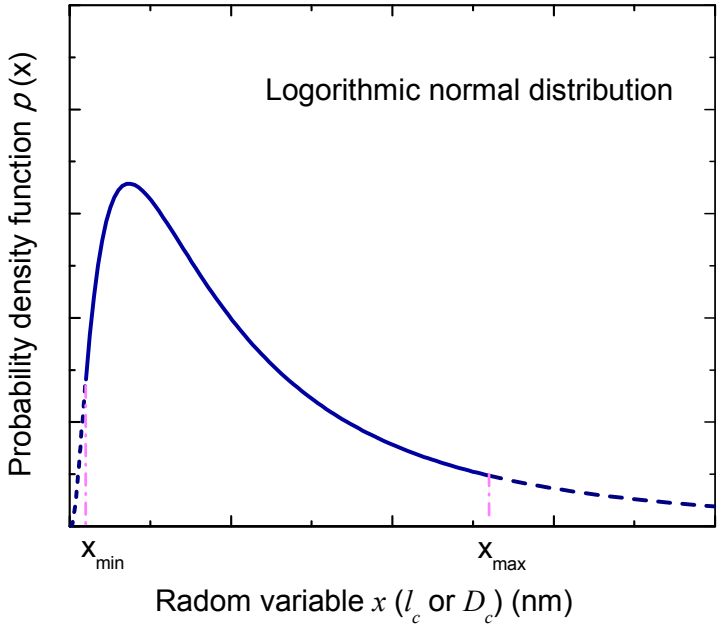

Figure 4: Illustration of the actual upper and lower boundaries of the equivalent length and diameter of CNT clusters with the lognormal distribution.

Since the equivalent length and diameter of CNTs are closely related with the volume fraction of CNTs, α_l and α_D was assumed to change with the volume fraction. The depending relationship of them on the volume fraction are still unknown, however, they can be evaluated by using the polynomial function interpolation method to numerically fit the real nonlinear curves. Based on the experimental stress-strain curves at four different volume fractions [9], the cubic spline function was used to match these data points, then α_l can be expressed as:

$$\alpha_l = b(v_f)l = (a_1 v_f^{\,3} + b_1 v_f^{\,2} + c_1 v_f)l \tag{22}$$

Since the change of α_D with volume fraction $(0 \le v_f < 1)$ is faster than α_l and the change of β_D is also faster than β_l, then α_D and β_D can be expressed by a quadric polynomial interpolation function:

$$\alpha_D = g\left(v_f\right)D = \left(a_2 v_f^4 + b_2 v_f^3 + c_2 v_f^2\right)D \tag{23}$$

Finally, by substituting Eqs. (20-23) into Eq. (15) and then into Eq. (1) together with Eq. (10), we can get the modified micromechanical model of CNT reinforced metal matrix composites to describe their thermo-viscoplastic flow behaviors:

$$\begin{aligned}\sigma_c = \mathrm{R}(\theta_f)\left\{1-\frac{D}{l}\frac{(a_2 v_f^{\,2} + b_2 v_f + c_2)}{(a_1 v_f^{\,2} + b_1 v_f + c_1)} v_f \left[\left(\frac{1}{\sqrt{v_f}} - 1\right)\cdot\frac{E_f}{G_m}\right]^{1/2}\right\} v_f \sigma_f + \\ (1-v_f)\left\{\sigma_{ath} + \hat{Y}\varepsilon^n \exp\left[\xi_1 T \ln\left(\frac{\dot{\varepsilon}}{\dot{\varepsilon}_{s0}}\right)\right]\left\{1-\left[-\xi_2 T \ln\left(\frac{\dot{\varepsilon}}{\dot{\varepsilon}_0}\right)\right]^{1/q}\right\}^{1/p}\right\}\end{aligned} \tag{24}$$

DETERMINATION OF MODEL PARAMETERS

Aluminum and its alloys are widely used in aerospace and automotive industries because of their good mechanical properties [27]. CNTs can be an ideal reinforcement to design aluminum matrix nanocomposites (CNT/Al) to improve their wear and creep properties. So a typical CNT-reinforced MMNC (CNT/Al) is chosen as the example in this paper.

Determination of model parameters for pure aluminum matrix

As the matrix model is relatively independent to the strengthening component in the composite model, the material parameters in the matrix model in Eq. (10) can be determined firstly. For the pure aluminum matrix, the two reference strain rates $\dot{\varepsilon}_{s0}$ and $\dot{\varepsilon}_0$ can be evaluated in advance. The two parameters lie in logarithmic functions and produce a smaller influence than ξ_1 and ξ_2 together with them. So their evaluation errors can be offset by fitting of ξ_1 and ξ_2. The value of $\dot{\varepsilon}_0$ is evaluated as $1\times10^7 s^{-1}$, and the value of $\dot{\varepsilon}_{s0}$ can be estimated as $1\times10^9 s^{-1}$ which is generally two orders greater than $\dot{\varepsilon}_0$.

The remaining seven parameters, σ_{ath}, $\hat{Y}$, n, ξ_1, ξ_2, p, q, can be determined by a global multi-variables nonlinear optimization method, i.e. generic algorithm (GA) as used in [23], based on a group of experimental stress-strain curves of pure aluminum [9, 28] at different strain rates and temperature. A Matlab program has been developed to realize the optimization calculations. The optimized results of the matrix model parameters were listed in Table 1.

Model Parameters	Theoretically allowed ranges	optimized results	units
σ_{ath}	[0, 20]	12.0	MPa
$\hat{Y}$	[100, 1000]	456	MPa
n	[0, 1]	0.293	/
ξ_1	$[9\times10^{-6}, 9\times10^{-5}]$	1.11×10^{-5}	1/K
ξ_2	$[9\times10^{-6}, 9\times10^{-5}]$	1.04×10^{-5}	1/K
p	(0, 1]	0.939	/
q	[1, 2]	1.712	/

Table 1: Optimized results of the material parameters of the Al matrix model

Determination of model parameters for CNT/Al composite

For the CNT/Al composite in [9], the average original length and diameter of CNTs can be known as $\bar{l}_0 = 1\mu m$ and $\bar{D}_0 = 25nm$. The CNT strength parameters in the composite model of Eq. (24) can be first ascertained as $\sigma_f = 30GPa$ and $\sigma_{fb} = 100GPa$ [29]. The shear yield strength of perfect bonding interface should be equal to that of the matrix, $\tau_{i,y} = 45MPa$. The parameters in the distribution function of misorientation angle were evaluated as $B = 0.874$ and $k = 6.47$. The CNT weight fractions were transformed into volume fractions by using the measured density, and the congruent relationship of weight fractions and volume fractions for CNT/Al was listed in Table 2.

Weight fractions $wt(\%)$	0	0.5	1.5	2.0
Measured density $\rho(g/cm^3)$	2.636	2.642	2.638	2.625
Volume fractions $v_f(\%)$	0	0.68	1.88	3.12

Table 2: The congruent relationship of volume fractions and weight fractions for CNT/Al

The remaining seven parameters, (a_1, b_1, c_1, a_2, b_2, c_2, θ_f), were determined based on the experimental stress-strain curves of CNT/Al composite [9] at different volume fractions, by using the same optimization method as mentioned above. The physically available ranges of these parameters were ascertained by the cubic spline interpolation curve matching. The optimized constitutive parameters of the CNT/Al composite were finally shown in Table 3.

Model parameters	a_1	b_1	c_1	a_2	b_2	c_2	θ_f
Varying ranges	[2.5e5, 2.5e6]	[-4.5e4, -5e3]	[100, 900]	[1.5e7, 3.5e7]	[-7e5, -3e5]	[6e3, 1.4e4]	$(55^\circ, 90^\circ)$
Optimized results	2.96×10^5	-1.35×10^4	873	3.1×10^7	-5.6×10^5	6030	62.6°

Table 3: Final optimized constitutive parameters of CNT/Al nanocomposite.

RESULTS AND DISCUSSION

In this section, the new model established and determined for the CNT/Al nanocomposite will be compared with experimental data for validation, and then some of important predictions of the new model will be presented.

Validation of the new model

As shown in Figure 5, the true stress-strain curves calculated from the proposed new model were compared with the experimental data obtained in compression tests [9] for CNT/Al composite of 0.68 %, 1.88 % and 3.12 % CNT volume concentrations. The curve of 0 % CNT composite namely corresponds to the pure aluminum matrix material. Obviously, the strength of the CNT/Al composite is effectively enhanced by the addition of CNTs at volume fractions of 0.68% and 1.88%. However, the strength of the composite drops at a higher volume concentration of 3.12 %, which should be caused by the presence of too many CNT clusters. It was indicated that the new model can well describe the true stress-strain relation of the composite at different volume fraction, especially at large strain because that the new matrix model has the ability of reflecting the plasticity of composites during large deformation.

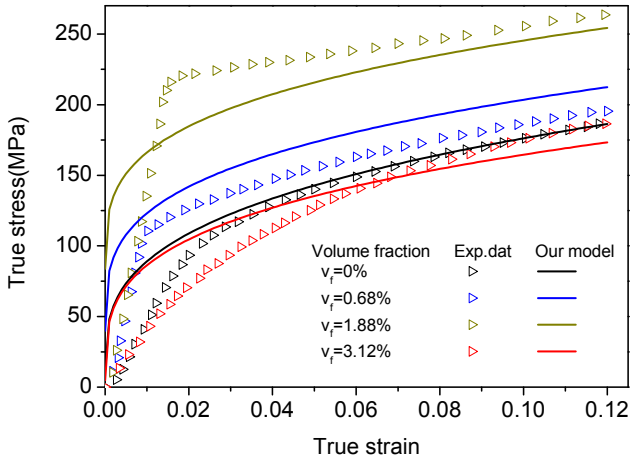

Figure 5: Comparison of the model description and experimental data [9] of the true stress-stain curves for CNT/Al composite at different volume fractions (under quasi-static loading and at room temperature).

The dependence of the flow stress of CNT/Al composite on the volume fraction at different strains was shown in Figure 6 so as to validate the new model based on experimental data [9]. It is obvious that there exists an extreme point in the strength of the composite with the variation of volume fraction. For the sample of CNT/Al composite, its strength gets the maximum value at about 2.0 vol.% in experiments, and the model prediction of the maximum strength appears at 2.5 vol.%, showing a certain error with the experimental result but well describing the varying trend of the experimental data

within the whole range of volume fraction. Obviously, the strength of the composite increases with the increasing volume fraction at relatively lower volume fractions, and then begins to drop when the volume fraction exceeds a critical point. The reason for this noticeable phenomenon should be resulted from the cluster effect of CNTs which varies with volume fraction. The number of CNT clusters dramatically goes up at higher volume fraction for a large amount of CNTs tend to entangle in the matrix, which is definitely detrimental to the mechanical properties of the composites.

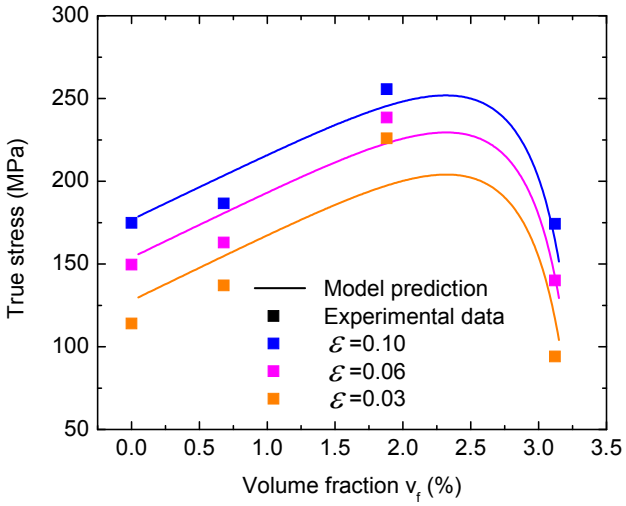

Figure 6: Model validation by the experimental data [9] of the dependence of the flow stress of CNT/Al composite on the volume fraction at different strains (under quasi-static loading and at room temperature).

The predictions of the basic model [13] which does not consider the cluster effect as well as misorientation angle were presented in Figure 7 at the volume fractions of 0.68 %, 1.88 % and 3.12 %, so as to demonstrate the correctness of the new model modified. It can be seen that the predicting curves monotonously increase with the increasing volume fraction of CNTs, and that the predictive values at 3.12 vol.% are much higher than those of the experimental results in [9]. This is mainly caused by the ignorance of the cluster effect and imperfect interface influence in the basic model. The interfacial bonding between pure aluminum and CNTs will be weaken due to the agglomeration of CNTs, as a consequence, the effective load transfer between the Al matrix and CNTs will be seriously obstructed on the imperfect interface. Thus, compared with the traditional model, it is obvious that the new model with consideration of the cluster effect can give satisfactory predictions.

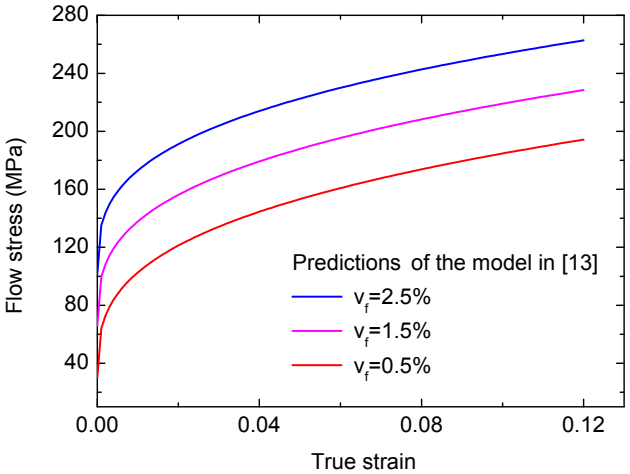

Figure 7: The predictions of the basic model [13] without consideration of the cluster effect and misorientations at different volume fractions under quasi-static loading and at room temperature.

Model predictions and discussion

The dependence of the model prediction of direct strengthening of CNT/Al composite on the average aspect ratio of the primary length to diameter of CNTs (l / D) was given in Figure 8 at a strain of 0.04. It can be seen in the figure that the

strengthening stress nonlinearly goes up with the increasing aspect ratio. The significant increase in strengthening with increasing length is obvious when the aspect ratio is less than 50 (or CNT length is less than 1 μm at a given CNT diameter of 20 nm). However, the curve tends to an asymptote when the CNT length is greater than 1 μm. In other words, beyond a critical length, the strengthening effect reaches a saturated value, which is consistent with the fact that the clustering of CNTs rapidly increases with increasing aspect ratio. In addition, the strengthening increases with the decreasing CNT diameter at a given CNT length, as found in [15] with perfect bonding interface.

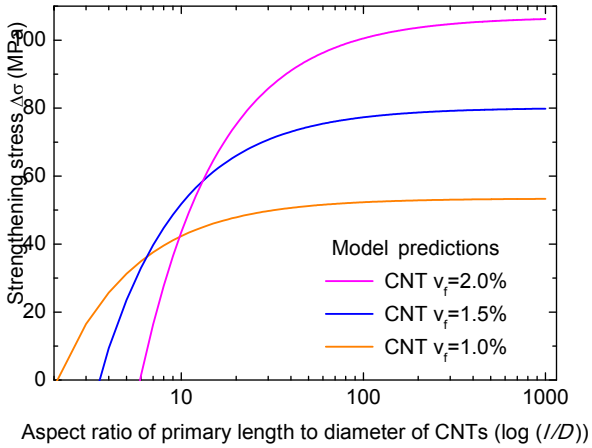

Figure 8: The dependence of the strengthening stress of CNT/Al composite on the average aspect ratio of primary length to diameter of CNTs under different volume fractions at a strain of 0.04.

The new model's predictions of the dependence of flow stress of the CNT/Al composite on temperature at different volume fractions were presented under quasi-static and dynamic loading and at a strain of 0.04 in Figure 9. A wide temperature range from low temperature (50K) to high temperature (1000K) was provided for the wide application conditions of MMNCs. When the volume fraction of CNTs is equal to 1.88 %, the flow stress under quasi-static loading descends about 75 MPa from room temperature to high temperature. And the flow stress of the CNT/Al composite under high-strain-rate loading is about 80 MPa higher than that at quasi-static loading.

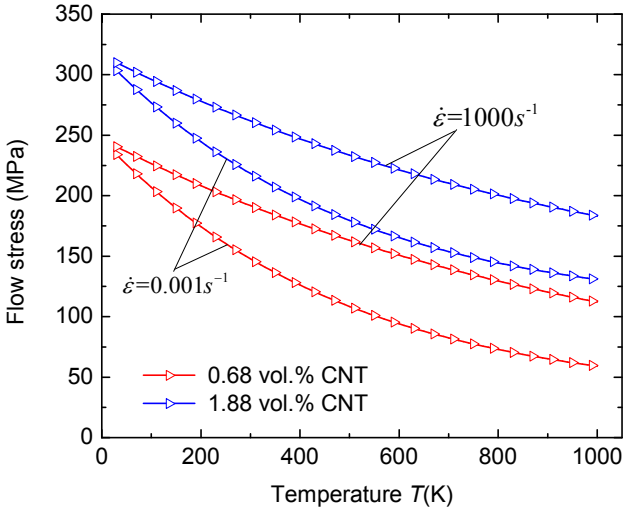

Figure 9: Dependence of the flow stress of CNT/Al composite on temperature at different volume fractions under quasi-static and dynamic loading.

The strain rate sensitivities of the flow stress of the CNT/Al composite at different volume fractions were predicted under room and high temperature and at a strain of 0.04 in Figure 10. It was indicated that the ascending trend of the flow stress with increasing logarithmic strain rate is basically linear at room temperature and somewhat nonlinear at high

temperature. The flow stress of CNT/Al composite will increase about 50-60 MPa from $10^{-3}s^{-1}$ to $10^{3}s^{-1}$, with a similar growth ratio to pure aluminum. Thus, the strain rate effect of CNT-reinforced MMNCs during plastic deformation should mainly be reflected in the metal matrix materials.

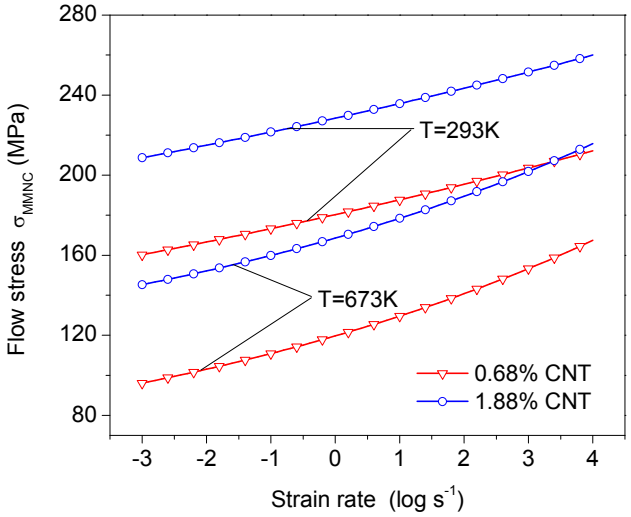

Figure 10: Strain rate sensitivities of the flow stress of CNT/Al composite at different volume fractions under room and high temperature.

CONCLUSIONS

In this paper, we have developed a new micromechanical constitutive model to capture the overall elasto-plastic response of carbon nanotube reinforced metal matrix nanocomposites. The significant influences of CNT clusters and misorientations on the mechanical properties of the nanocomposites were considered in the proposed model. The cluster effect was introduced into the new model by using the statistically-averaged equivalent length and diameter of CNT clusters with a logarithmic normal distribution, and the misorientation angle was considered by using an improved physically-based strength model of short fibre-reinforced composites.

For the CNT/Al nanocomposite, the new model was validated by experimental results first, and was also compared with the traditional model without considering the cluster effect. It was demonstrated that the new model is reasonable and reliable. The predictions of the new model of the CNT/Al nanocomposite indicated that the strengthening stress nonlinearly goes up with the increasing aspect ratio of the length to diameter of CNTs and eventually tends to a saturated value. In addition, the flow stress of the composite descends with increasing temperature under quasi-static and dynamic loading, while ascends with the increasing logarithmic strain rate basically linearly at room temperature and somewhat nonlinearly at high temperature.

ACKNOWLEDGEMENTS

This research work was supported by the National Natural Science Foundation of China (No. 11272286), the Zhejiang Provincial Natural Science Foundation of China for Distinguished Young Scholars (LR13E050001) and the Open Foundation of State Key Lab of Explosion Science and Technology of China (No. KFJJ14-9M).

REFERENCES

[1] Jarali, C.S., Patil, S.F., Pilli, S.C., Lu, Y.C., Modeling the effective elastic properties of nanocomposites with circular straight CNT fibers reinforced in the epoxy matrix, J Mater Sci., 48 (2013) 3160-3172.

[2] Wang, X., Yong, Z.Z., Li, Q.W., Bradford, P.D., Liu, W., Tucker, D.S., Cai, W., Wang, H., Yuan, F.G., Zhu, Y.T., Ultrastrong, Stiff and Multifunctional Carbon Nanotube Composites, Mater Res Lett., 1 (2013) 19-25.

[3] Dastgerdia, J.N., Marquis, G., Salimi, M., Micromechanical modeling of nanocomposites considering debonding and waviness of reinforcements, Compos Struct., 110 (2014) 1-6.
[4] Sridhar, I., Narayanan, K.R., Processing and characterization of MWCNT reinforced aluminum matrix composites, J Mater Sci., 44 (2009) 1750-1756.
[5] Habibi, M.K., Paramsothy, M., Hamouda, A.M.S., Gupta, M., Enhanced compressive response of hybrid Mg–CNT nano-composites, J Mater Sci., 46 (2011) 4588-4597.
[6] Salimi, S., Izadi, H., Gerlich, A.P., Fabrication of an aluminum–carbon nanotube metal matrix composite by accumulative roll-bonding, J Mater Sci., 46 (2011) 409-415.
[7] Joo, S.H., Yoon, S.C., Lee, C.S., Nam, D.H., Hong, S.H., Kim, H.S., Microstructure and tensile behavior of Al and Al-matrix carbon nanotube composites processed by high pressure torsion of the powders, J Mater Sci., 45 (2010) 4652-4658.
[8] Rawal, S., Metal-Matrix Composites for Space Applications, JOM., 53 (2001) 14-17.
[9] Yang, X.D., Shi, C.S., He, C.N., Liu, E.Z., Li, J.J., Zhao, N.Q., Synthesis of uniformly dispersed carbon nanotube reinforcement in Al powder for preparing reinforced Al composites, Compos: Part A., 42 (2011) 1833-1839.
[10] Liao, J.Z., Tan, M.J., Sridhar, I., Spark plasma sintered multi-wall carbon nanotube reinforced aluminum matrix composites, Mater & Design., 31 (2010) 96-100.
[11] Kim, K.T., Cha, S., Hong, S.H., Hong, S.H., Microstructures and tensile behavior of carbon nanotubes reinforced Cu matrix nanocomposites, Mater Sci and Eng A., 430 (2006) 27-33.
[12] Li, H., Misra, A., Horita, Z., Strong and ductile nanostructured Cu-carbon nanotube composite, Appl Phys Lett., 95 (2009) 071907.
[13] Courtney, T.H., Mechanical Behavior of Materials, McGraw-Hill Book Co., Singapore. (2000).
[14] Ryu, H.J., Cha, S.I., Hong, S.H.J., Generalized shear-lag model for load transfer in SiC/Al metal-matrix composites, Mater Res., 18 (2003) 2851-2858.
[15] Barai, P., Weng, G.J., A theory of plasticity for carbon nanotube reinforced composites, Int J Plasticity, 27 (2011) 539-559.
[16] Morsi, K., Esawi, A., Effect of mechanical alloying time and carbon nanotubes (CNT) content on the evolution of aluminum (Al)–CNT composite powders, J Mater Sci., 42 (2007) 4954-4959.
[17] Kwon, H.S., Park, D.H., Silvain, J.F., Kawasaki, A., Investigation of carbon nanotube reinforced aluminum matrix composite materials, Compos Sci Technol., 70 (2010) 546-550.
[18] Esawi, A.M.K., Borady, M.A.E., Carbon nanotube-reinforced aluminum strips, Compos Sci Technol., 68 (2008) 486-492.
[19] Coleman, J.N., Cadek, M., Blake, R., Nicolosi, V., Ryan, K.P., Belton, C., Fonseca, A., Nagy, J.B., Gunko, Y.K., Blau, W.J., High-Performance Nanotube-Reinforced Plastics: Understanding the Mechanism of Strength Increase, Adv Funct Mater., 14(8) (2004) 791-798.
[20] Villoria, R.G., Miravete, A., Mechanical model to evaluate the effect of the dispersion in nanocomposites, Acta Mater., 55 (2007) 3025-3031.
[21] Johnson, W.G., Gilman, J.J., Dislocation velocities, dislocation densities, and plastic flow in lithium fluoride crystals, J Appl Phys., 30 (1959) 129-144.
[22] Kocks, U.F., Argon, A.S., Ashby, M.F., Thermodynamics and kinetics of slip, Prog Mate Sci, 19 (1975) 1-281.
[23] Gao CY, Zhang LC. A constitutive model for dynamic plasticity of FCC metals, Mater Sci Eng A., 527 (2010) 3138-3143.
[24] Zhu, Y.T., Blumenthal, W.R., Lowe, T.C., The tensile strength of short fibre-reinforced composites, J Mater. Sci., 32 (1997) 2037-2043.
[25] Luo, Z.P., Koo, J.H., Quantifying the dispersion of mixture microstructures, J Microscopy, 225 (2007) 118-125.
[26] Tyson, B.M., Al-Rub, R.K.A., Yazdanbakhsh, A., Grasley, Z., A quantitative method for analyzing the dispersion and agglomeration of nano-particles in composite materials, Compos: Part B, 42 (2011) 1395-1403.
[27] Surappa, M.K., Aluminium matrix composites: Challenges and opportunities, Sadhana, 28 (2003) 319-334.
[28] Kima, W.J., Lee, S.H., High-temperature deformation behavior of carbon nanotubes (CNT)-reinforced aluminum composites and prediction of their high-temperature strength, Compos: Part A., 67 (2014) 308-315.
[29] Cha, S.I., Kim, K.T., Arshad, S.N., Mo, C.B., Hong, S.H., Extraordinary strengthening effect of carbon nanotubes in metal matrix nanocomposites processed by molecular level mixing, Adv Mater, 17 (2005) 1377-1381.